

MINIMUM JERK REACHING MOVEMENTS OF HUMAN ARM WITH MECHANICAL CONSTRAINTS AT ENDPOINT

Daohang Sha^a, Jim Patton^b, and Ferdinando. A. Mussa-Ivaldi^b

^a McPhail Equine Performance Center, College of Veterinary Medicine,
Michigan State University, East Lansing, MI 48824, USA
shadaoha@cvm.msu.edu

^b Sensory Motor Performance Program, Rehabilitation Institute of Chicago and Northwestern University,
345 E Superior St. Chicago, IL 60611, USA
j-patton@northwestern.edu, sandro@northwestern.edu

ABSTRACT

In this paper, minimum jerk movement on the constrained sphere was studied by using both theoretical analysis and experimental investigation. Based on the constraint optimal principle, it was obtained that the trajectory of the minimum jerk movement on the surface of sphere should be a geodesic. Experiments used a robot especially designed for studies of human-machine interactions to evaluate movements on a virtual surface. Experiments revealed that the nervous system tries to learn and represent a constrained surface so it can move most efficiently (i.e. move along a geodesic) with practice, and that subjects can generalize this knowledge to nearby locations not yet visited.

Keywords: motor learning, haptics, robot.

1. INTRODUCTION

Kinematically constrained movements are a daily experience. For example, driving a car by turning the steer wheel or opening a door by pulling on the doorknob is a constrained movement by the nature of hinges, i.e. the steer wheel and the doorknob must move along a circular path. When our hands move on a surface such as a tabletop, any excessive forces against the surface are counterproductive. Fast movements along a surface to a target require rapid feedback and extremely precise sensors, and can easily exceed physiological limits. Alternatively, through repeated movements on a surface, one might acquire knowledge of its shape so that movements can be efficiently pre-planned. This study examines the prospect that the nervous system learns to represent such a constraint surface so it can move most efficiently. To determine whether this is the case, we extend some of the following principles of smoothness and adaptation to the more general case in which the hand interacts mechanically with a surface.

Early observations by Morasso showed that, when reaching for a target, subjects tend to move their hand along a straight path, with a symmetric, bell-shaped, velocity profile (Morasso, 1981). This is not as trivial an observation as it first appears – these simple movements of the hand require rather complex patterns in the joints, and the same joint excursions starting from different initial positions lead to different hand displacements. Morasso's finding is consistent with Bernstein's more general notion that the motor system is able to coordinate multiple degrees of freedom into simple movements of the "end-effector" (Bernstein, 1967). These kinematics cannot be attributed to visual perception: even those who are blind from birth exhibit the same patterns (Miall and Haggard, 1995; DiZio and Lackner, 2000).

Several studies on humans have identified the relationship between these spatial-temporal characteristics and smoothness. A smooth movement can be defined mathematically as a movement in which higher derivatives are kept to an overall minimum. Flash and Hogan proposed the simple optimization principle that the motor system strives to achieve maximally smooth movements, could account multi-joint movements (Flash and Hogan, 1985). Specifically, their approach minimized the first temporal derivative of acceleration, or "jerk" while constraining all higher derivatives to zero. Their approach was only applicable to two-dimensional space, however. Other theoretical analysis and

experiments have demonstrated the tendencies toward smoothness in human arm movements (Flash and Hogan, 1985; van Donkelaar *etc.*, 1992). Similar results have been found by minimizing the overall torque-rate-of-change (Uno *etc.*, 1989; Kawato *etc.*, 1990). This is not surprising, since Newton's second law states that jerk is proportional to the rate of change of force, and force is related to joint torque via the Jacobian. However, the principle of minimizing torque-rate-of-change is hard to reconcile with the observation that when the hand is exposed to changes in limb/environment dynamics, subjects recover the smooth kinematics of the hand by modifying the time course of the joint torques.

Constraining surfaces can be considered as force fields, exerting reaction forces that prevent or limit motions inside the surfaces. For compliant surfaces, one may simply move his hand in a straight line and deform the surface as one moves along. With more rigid surfaces, penetrating becomes more difficult and the hand path must change. If subjects cannot cancel the constraining forces make a smooth and straight trajectory of the hand generate a motion on the surface. When it does, what is the resulting movement along the surface? One possible hypothesis is that the minimum jerk hypothesis still holds, yet subject to a constraint. However, in order to accomplish such a movement, one must plan movements based on some internal representation of the constraining surface's geometry.

In this paper, we make an initial attempt to determine whether the nervous system tries to learn and represent a constraint surface so it can move most efficiently by using theoretical simulation and experimental method. First, we develop a general framework for calculating the minimum-jerk trajectory on a constraining surface. Next, we present experiments that used a robot especially designed for studies of human-machine interactions to evaluate movements on a virtual surface. Our results support the hypothesis that repeated mechanical interaction with a constraining surface leads to movements that more closely resemble the minimum jerk trajectory, even for unpracticed directions.

2. METHODS

2.1 Theoretical Solution to the Minimum Jerk Movement on Surface

Jerk is mathematically defined as the rate of change of acceleration. Flash and Hogan (1985) used the time integral of the square of the magnitude of jerk to the 2-dimensions reaching movements. Extending this to the more general optimization problem of minimizing jerk in three dimensions while constrained to a surface, and applying the Lagrangian principle, we obtain the cost function

$$C = \int_0^{t_f} \left[\left(\frac{d^3x}{dt^3} \right)^2 + \left(\frac{d^3y}{dt^3} \right)^2 + \left(\frac{d^3z}{dt^3} \right)^2 + \lambda g(x, y, z) \right] dt, \quad (1)$$

where λ is a Lagrangian multiplier, $g(x, y, z) = 0$ is the equation of constraint surface.

We want to find the constrained trajectory that minimizes the cost function (1), which means there is a minimum jerk during the movement from point to point along the certain path. To minimize C , the problem will be led to solve an 18th-order ODEs (three correlative 6th-order ODEs, see Appendix) with 18 boundary conditions, i.e. positions, velocities and accelerations of endpoint at initial and final movement in three dimensions are zeros. Such problems are called *two-point boundary-value problems*, they are sometimes rather difficult to solve, even with a high-speed computer (Carignan and Cleary, 2000). A general analytical solution is not possible do to the unspecified shape of the surface. We used MATLAB function BVP4C which is especially designed for numerically solving two-point boundary value problems for ODEs by collocation. This method was tested by evaluating a minimum-jerk trajectory for a problem in which we knew the solution – a point-to-point movement on a sphere. It is well known that the shortest path between two points on a sphere is the geodesic, formed by passing a plane through the center of the sphere $(0, 0, 0)$ and two points (x_s, y_s, z_s) , (x_f, y_f, z_f) . These validation solutions did converge to the geodesic with a bell-shaped velocity profile resembling motions on the plane (see Fig.2, top left).

2.2 Experimental Tests

Twenty-five right-handed healthy subjects participated in the experiments: fifteen males and ten female, age 31-37. A robot (PHANToM robot with GHOST software development kit, SensAble Technologies, see Fig.1 (Salisbury and Srinivasan, 1997) especially designed for studies of human-machine interactions provided an object-oriented programming environment for force-feedback haptic interface (Carignan and Cleary, 2000). Position and forces of handle were sampled at 100Hz. The haptic service loop was updated at a 1kHz to ensure stability and a responsive interface. A virtual semi-sphere surface (radius of 200mm, stiffness 1Nmm⁻¹, and no dry friction or damping) was used as the haptic surface. Subjects were

seated in front of the robot and gripped the handle. Subjects were only instructed to move their hand from one point to another point without telling them they were moving on the sphere. At the beginning of experiments, two targets were presented at left side 30° for 60 trials about one minute. Then two targets were presented at right side 30° for 360 trials about five minutes for training. Subjects could rest at any time during the training phase. After training period, go back to left side for 60 trials about one minute. A tone signaled them to begin the next movement and also served as feedback to control the speed of movements. This tone indicated that the movement was too fast with a high pitch (4500Hz), too slow with a low pitch (250Hz), or satisfactory speed with a medium pitch (2500Hz) if the speed is within a tolerable range of 0.6 to 0.8 m.s^{-1} . Movements were separated using speed thresholds (above 0.005 m.s^{-1}).

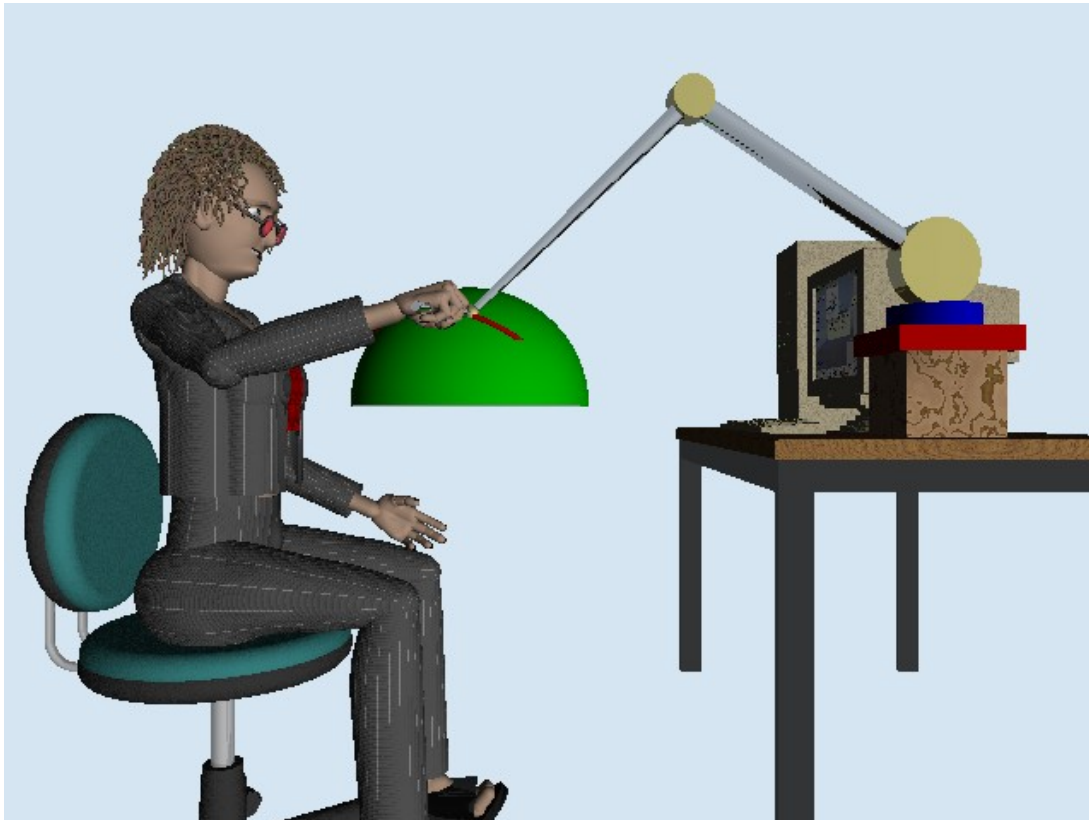


Figure 1 Experimental apparatus for the generation of virtual surfaces. The subject is grasping the handle of a Phantom 3.0 (Sensable Tech.) that generates a force field corresponding to a spherical surface (not visible to the subject).

2.3 Data Analysis

We hypothesized that repeated mechanical interaction with a constraining surface leads to the implicit learning of its geometry, and hence (1) trajectories should become more like the minimum-jerk with practice, (2) contact forces should become smaller with practice, and (3) these results generalize to nearby, unpracticed trajectories.

To allow us to answer the questions described previously, first we will calculate the path error, which measures the length difference between the actual trajectory and the geodesic; second, we measure the root mean square error (RMSE) by applying a moving window to the data sequence. The width of the window is $n=30$. For each movement, the algorithm will find the start point and end point automatically, and then calculate the length of geodesic and trajectory. The too short or too long movements will be removed from the data sequence.

2.3.1 Shortest Distance between Two Points on the Sphere - Length of Geodesic

The distance between two locations on the sphere is not simply the length of the straight line connecting them. The surface of a sphere curves, and as a result, the line connecting two locations also curves. The great circle distance is the length of the SHORTEST arc on the surface of the sphere connecting the two locations that is the length of geodesic. First of all, we must know formulas for spherical coordinates

$$\begin{cases} x = r \cos(\theta) \sin(\gamma), \\ y = r \sin(\theta) \sin(\gamma), \\ z = r \cos(\gamma), \end{cases}$$

where r is the radius of the sphere, γ is the longitude, and θ is the latitude of the point (x,y,z) . The sphere is located with its center at the origin. Given two points $a = (x_s, y_s, z_s)$ and $b = (x_f, y_f, z_f)$ on the sphere, one can find the angle between them from two formulas for the scalar product

$$a \cdot b = |a| |b| \cos(\alpha) = x_s x_f + y_s y_f + z_s z_f,$$

where $|a|$ is the distance from a to the origin (the length of the corresponding vector), or $\sqrt{x_s^2 + y_s^2 + z_s^2}$.

Now, it's like on a circle. One has to find the length of an arc on a circle of radius r subtending a given central angle α which is given by length

$$L_g = r\alpha = r \cos^{-1} \left(\frac{x_s x_f + y_s y_f + z_s z_f}{r} \right)$$

2.3.2 Mean Average Distance

Average distance between trajectory and geodesic can be calculated by

$$d_{avg} = \frac{1}{L_g} \sum_{n=1}^{n_f} d(nT_s) \cdot \Delta l(nT_s),$$

where T_s is the sample time; d is the length between trajectory and geodesic along the surface at the moment nT_s ; Δl is the length along the surface from the moment nT_s to $(n+1)T_s$; both d and Δl are calculated by the same formula as L_g is calculated.

The mean and the standard deviation of average distance are calculated by, respectively

$$\bar{d}_{avg}(i) = \frac{1}{n} \sum_{j=i-n/2}^{i+n/2-1} d_{avg}(i+j),$$

and

$$\Delta \bar{d}_{avg}(i) = \sqrt{\frac{1}{n-1} \sum_{j=i-n/2}^{i+n/2-1} [d_{avg}(i+j) - \bar{d}_{avg}(i)]^2},$$

where $i=n/2+1, \dots, N-n/2+1$, N is total number of movements, n is the width of a moving window on the data sequence.

2.3.3 Mean Average Constraint Forces

Assuming the coordinates of the contact point $(x_{i,j}, y_{i,j}, z_{i,j})$ and the contact forces $F_x(i, j), F_y(i, j)$, and $F_z(i, j)$, one obtains the constraint force by projecting the contact force onto the radial direction pass through center and contact point, i.e.

$$\begin{aligned} F_{cx}(i, j) &= F_x(i, j) \cos \left[\cos^{-1} \left(\frac{x(i, j)}{r} \right) \right], \\ F_{cy}(i, j) &= F_y(i, j) \cos \left[\cos^{-1} \left(\frac{y(i, j)}{r} \right) \right], \\ F_{cz}(i, j) &= F_z(i, j) \cos \left[\cos^{-1} \left(\frac{z(i, j)}{r} \right) \right]. \end{aligned}$$

So the average constraint force of each movement is sum of these projection and divided by the number of samples

$$F_{ac}(i) = \frac{1}{N} \sum_{j=1}^N [F_{cx}(i, j) + F_{cy}(i, j) + F_{cz}(i, j)]$$

The mean and the standard deviation of average constraint force are calculated by, respectively

$$\bar{F}_{ac}(i) = \frac{1}{n} \sum_{j=i-n/2}^{i+n/2-1} F_{ac}(i+j),$$

and

$$\Delta \bar{F}_{ac}(i) = \sqrt{\frac{1}{v-1} \sum_{j=i-n/2}^{i+n/2-1} [\bar{F}_{ac}(i+j) - \bar{F}_{ac}(i)]^2}.$$

2.3.4 Learning Rate

The change rate is used to explain the effects of learning and generalization, which is calculated by

$$\eta = \frac{x_I - x_F}{x_I},$$

where variable x represents average distance \bar{d}_{avg} or average constraint force \bar{F}_{ac} , subscript I means initial value and F means final value.

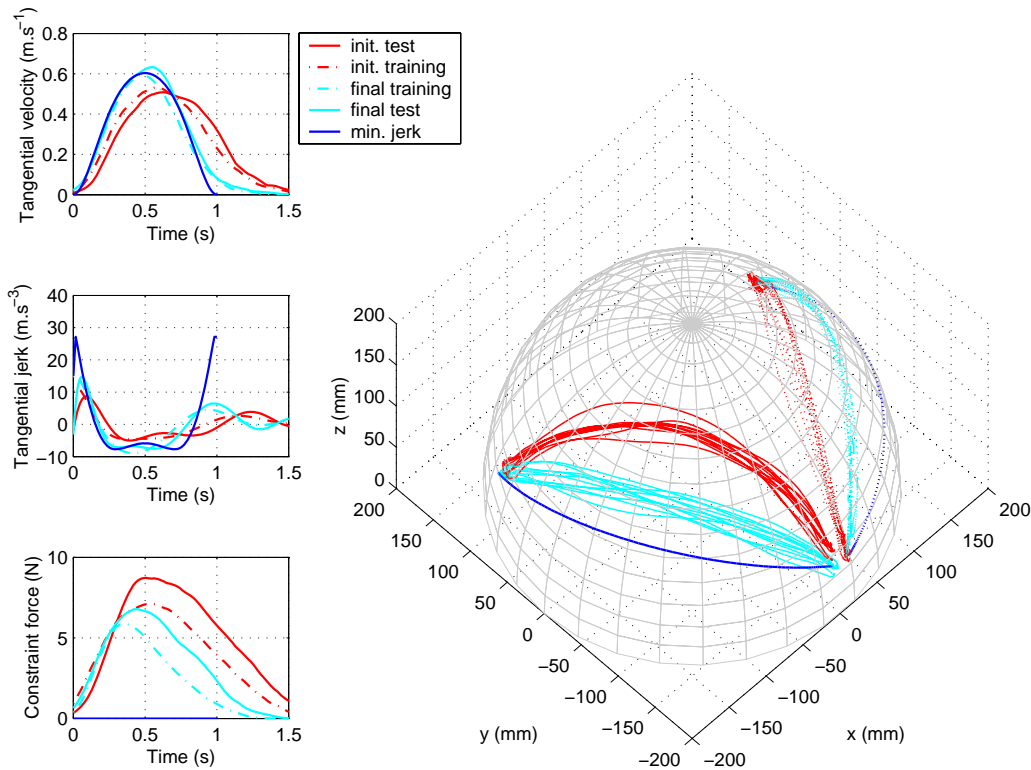


Figure 2 Training and test results for a subject's movement on the half-sphere: trajectories on the sphere and the average tangential velocity, jerk and constraint force

3. RESULTS AND DISCUSSION

The results of a typical experiment for individual subject are show in Fig.2 and Fig.3. Trajectories, tangential velocities, jerks and constraint forces are shown in Fig.2. Mean velocity profile looks like the theoretical one (bell shape). Fig.3 shows the change trends of the distance between the trajectory and the

geodesic and the constraint force with the practice for the whole experiment and their statistical analysis at the beginning and the end of training and test.

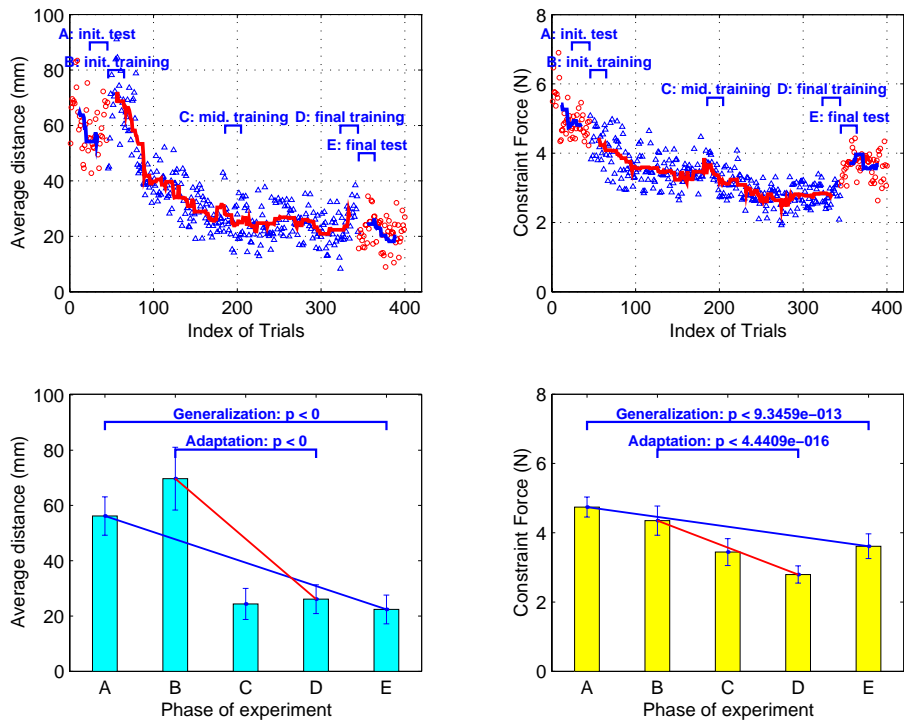


Figure 3 Individual subject's average distance and constraint force learning curves and statistical analysis

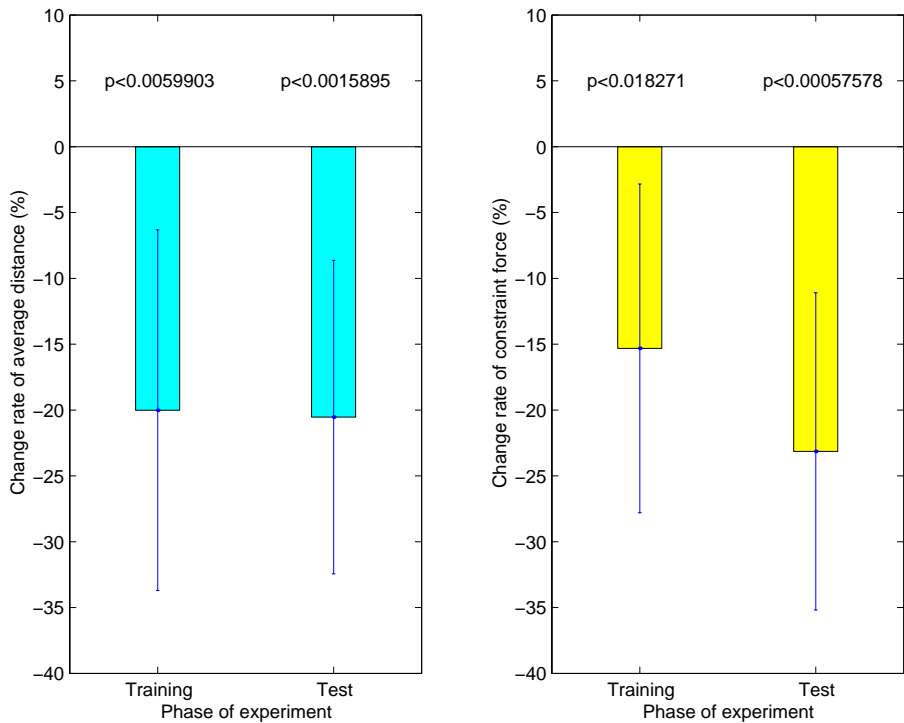


Figure 4 Group average learning rate at training and generalization rate at test

Across all subjects (see Fig. 4), we found that a) the average distance from the actual geodesic path (“geodesic distance”) decreased by 20% on the training trajectory and by 21% on the test trajectory; these changes were highly significant ($p < 0.006$); b) the mean contact force decreased by 15% on the training trajectories and by 23% on the test trajectories with both changes being mildly significant ($p < 0.02$); c) the changes in contact force and in geodesic distance were statistically independent; d) while there was a reduction in geodesic distance, this variable did not converge to zero (Fig. 2); These results suggest that subjects are forming an internal representation of the constraint, as they learn to reduce the error to geodesic and the contact forces.

Our results for this initial study support the hypothesis that repeated mechanical interaction with a constraining surface leads to movements that more closely resemble the minimum jerk trajectory, even for unpracticed directions. This suggests an internal representation of surface geometry. However, movement kinematics appeared to deviate systematically and significantly from those predicted by jerk optimization. The optimization of smoothness while reflecting the geometrical properties of Euclidean free space may not apply to movements constrained by curved surfaces.

4. CONCLUSIONS

Theoretical analysis has proved that the kinematic trajectories of the minimum jerk reaching movement on the surface of sphere is the shortest arc (geodesic) on the surface of the sphere between two locations. Also experimental investigation reveal that the trajectory of reaching movement will become more like the most efficient as practice, i.e. will be close to a geodesic and nervous systems can transfer the learning results to nearby locations not yet visited. It is emphasized that the research results which were presented in this paper are only the primary. The further work needs to be done. The next step will be to find out the effects of virtual texture, such as stiffness, damping of the virtual surface, on the learning of nervous system; the affections of movement speed on the learning of nervous system; adaptation of nervous system to the perturbation of the 3D surface; and distinguishing of surfaces etc.

APPENDIX: MINIMUM-JERK SOLUTION OVER SURFACE

1 Optimal Principle

We want to find the constrained trajectory that minimizes the cost function (1), which means there is a minimum jerk during the movement from point to point along the certain path. Generally, for any function $x(t)$, which is sufficiently differentiable in the interval $0 \leq t \leq t_f$, and for any performance index

$L(t, \dot{x}, \ddot{x}, \dots, \frac{d^n x}{dt^n})$ can be integrated over the same interval, the unconstrained cost function is described as

$$C(x) = \int_0^{t_f} L(t, \dot{x}, \ddot{x}, \dots, \frac{d^n x}{dt^n}) dt.$$

Assumes an extreme existing when $x(t)$ is the solution of Euler-Poisson equation (Bryson and Ho, 1975), we have

$$\frac{\partial L}{\partial x} - \frac{d}{dt} \left(\frac{\partial L}{\partial \dot{x}} \right) + \dots + (-1)^n \frac{d^n}{dt^n} \left(\frac{\partial L}{\partial x^n} \right) = 0.$$

Since in our case

$$L = \left(\frac{d^3 x}{dt^3} \right)^2 + \left(\frac{d^3 y}{dt^3} \right)^2 + \left(\frac{d^3 z}{dt^3} \right)^2 + \lambda g(x, y, z),$$

the necessary conditions for the problem are

$$\begin{cases} -\frac{d^3}{dt^3}\left(\frac{d\ddot{x}^2}{d\ddot{x}}\right) + \lambda \frac{\partial g}{\partial x} = 0, \\ -\frac{d^3}{dt^3}\left(\frac{d\ddot{y}^2}{d\ddot{y}}\right) + \lambda \frac{\partial g}{\partial y} = 0, \\ -\frac{d^3}{dt^3}\left(\frac{d\ddot{z}^2}{d\ddot{z}}\right) + \lambda \frac{\partial g}{\partial z} = 0, \end{cases}$$

that is

$$\begin{cases} -2\frac{d^6x}{dt^6} + \lambda \frac{\partial g}{\partial x} = 0, \\ -2\frac{d^6y}{dt^6} + \lambda \frac{\partial g}{\partial y} = 0, \\ -2\frac{d^6z}{dt^6} + \lambda \frac{\partial g}{\partial z} = 0. \end{cases} \tag{2}$$

From the third of above equation, one obtains

$$\lambda = 2\left(\frac{\partial g}{\partial z}\right)^{-1} \frac{d^6z}{dt^6}$$

Substitute λ into the first two equations of (2), one finally obtains

$$\begin{cases} \frac{d^6x}{dt^6} - \left(\frac{\partial g}{\partial z}\right)^{-1} \frac{d^6z}{dt^6} \frac{\partial g}{\partial x} = 0, \\ \frac{d^6y}{dt^6} - \left(\frac{\partial g}{\partial z}\right)^{-1} \frac{d^6z}{dt^6} \frac{\partial g}{\partial y} = 0, \end{cases} \tag{3}$$

2 Case Study: Movement on the Elliptic Surface

Let us consider a class of elliptic surface. As was known, when the length of three axis are equal, the elliptic surface will become spherical surface. Because the constraint equation is

$$g(x, y, z) = \frac{x^2}{a^2} + \frac{y^2}{b^2} + \frac{z^2}{c^2} - 1 = 0,$$

it is easy to get these derivatives directly from above equation, i.e.

$$\frac{\partial g}{\partial x} = \frac{2x}{a^2}, \frac{\partial g}{\partial y} = \frac{2y}{b^2}, \frac{\partial g}{\partial z} = \frac{2z}{c^2}.$$

Derive both sides of equation $\frac{z^2}{c^2} = 1 - \left(\frac{x^2}{a^2} + \frac{y^2}{b^2}\right)$ six times, one gets,

$$\begin{aligned} & \frac{1}{c^2} \left(15 \frac{d^4z}{dt^4} \frac{d^2z}{dt^2} + 10 \frac{d^3z}{dt^3} \frac{d^3z}{dt^3} + 6 \frac{dz}{dt} \frac{d^5z}{dt^5} + z \frac{d^6z}{dt^6} \right) \\ &= -\frac{1}{a^2} \left(15 \frac{d^4x}{dt^4} \frac{d^2x}{dt^2} + 10 \frac{d^3x}{dt^3} \frac{d^3x}{dt^3} + 6 \frac{dx}{dt} \frac{d^5x}{dt^5} + x \frac{d^6x}{dt^6} \right) \\ & - \frac{1}{b^2} \left(15 \frac{d^4y}{dt^4} \frac{d^2y}{dt^2} + 10 \frac{d^3y}{dt^3} \frac{d^3y}{dt^3} + 6 \frac{dy}{dt} \frac{d^5y}{dt^5} + y \frac{d^6y}{dt^6} \right). \end{aligned}$$

Rearrange above equation, one gets

$$\frac{d^6z}{dt^6} = -\frac{c^2x}{a^2z} \frac{d^6x}{dt^6} - \frac{c^2y}{b^2z} \frac{d^6y}{dt^6} + D,$$

where

$$D = -\frac{c^2}{a^2 z} \left(15 \frac{d^4 x}{dt^4} \frac{d^2 x}{dt^2} + 10 \frac{d^3 x}{dt^3} \frac{d^3 x}{dt^3} + 6 \frac{dx}{dt} \frac{d^5 x}{dt^5} \right) \\ - \frac{c^2}{b^2 z} \left(15 \frac{d^4 y}{dt^4} \frac{d^2 y}{dt^2} + 10 \frac{d^3 y}{dt^3} \frac{d^3 y}{dt^3} + 6 \frac{dy}{dt} \frac{d^5 y}{dt^5} \right) \\ - \frac{1}{z} \left(15 \frac{d^4 z}{dt^4} \frac{d^2 z}{dt^2} + 10 \frac{d^3 z}{dt^3} \frac{d^3 z}{dt^3} + 6 \frac{dz}{dt} \frac{d^5 z}{dt^5} \right).$$

Equation (3) becomes

$$\begin{cases} \frac{d^6 x}{dt^6} = \frac{c^2 x}{a^2 z} \frac{d^6 z}{dt^6}, \\ \frac{d^6 y}{dt^6} = \frac{c^2 y}{b^2 z} \frac{d^6 z}{dt^6}, \\ \frac{d^6 z}{dt^6} = -\frac{c^2 x}{a^2 z} \frac{d^6 x}{dt^6} - \frac{c^2 y}{b^2 z} \frac{d^6 y}{dt^6} + D. \end{cases}$$

It is easy to solve it,

$$\begin{cases} \frac{d^6 x}{dt^6} = \frac{c^2 x}{a^2 z} \left[1 + \left(\frac{c^2 x}{a^2 z} \right)^2 + \left(\frac{c^2 y}{b^2 z} \right)^2 \right]^{-1} D, \\ \frac{d^6 y}{dt^6} = \frac{c^2 y}{b^2 z} \left[1 + \left(\frac{c^2 x}{a^2 z} \right)^2 + \left(\frac{c^2 y}{b^2 z} \right)^2 \right]^{-1} D, \\ \frac{d^6 z}{dt^6} = \left[1 + \left(\frac{c^2 x}{a^2 z} \right)^2 + \left(\frac{c^2 y}{b^2 z} \right)^2 \right]^{-1} D. \end{cases}$$

REFERENCES

- Bernstein N, (1967) *The coordination and regulation of movement*. Oxford: Pergamon Press.
- Bryson, A. E., Ho, Y.-C., (1975) *Applied Optimal Control: Optimization, Estimation, and Control*, New York: Hemisphere Publishing Corporation, 1-127.
- Carignan, C. R., Cleary, K. R. (2000) Closed-loop force control for haptic simulation of virtual environments, *Haptics-e*, **1**(2), 1-14.
- DiZio P., Lackner J. (2000) Congenitally blind individuals rapidly adapt to Coriolis force perturbations of their reaching movements, *Journal of Neurophysiology*, **84**, 2175-2180.
- Flash, T., Hogan, N. (1985) The Coordination of Arm Movements: An Experimentally Confirmed Mathematical Model, *The Journal of Neuroscience*, **5**(7), 1688 -1703.
- Kawato M., Maeda Y., Uno Y., Suzuki R. (1990) Trajectory Formation of Arm Movement by Cascade Neural Network Model Based on Minimum Torque-Change Criterion., *Biological Cybernetics*, **62**, 275-288.
- Miall R., Haggard P., (1995) The curvature of human arm movements in the absence of visual experience, *Experimental Brain Research*, **103**, 421-428.
- Morasso P., (1981) Spatial control of arm movements, *Experimental Brain Research*, **42**, 223-227.
- Salisbury, J.K., Srinivasan, M.A., (1997) Phantom-based haptic interaction with virtual objects, *IEEE Comput. Graph. Appl.* **17**, 6-10.
- Uno, Y, Kawato M., Suzuki, R., (1989) Formation and control of optimal trajectory in human multijoint arm movement, *Biological Cybernetics*, **61**, 89-101.

van Donkelaar, P., Lee R.G., Gellman R.S. (1992) Control strategies in directing the hand to moving targets, *Exp Brain Res.*, **91**(1), 151-161.

Received: July 23rd 2003

Accepted in final format: December 28th 2004 after one revision

About the authors

Daohang Sha is a research associate at McPhail Equine Performance Center at Michigan State University. His researching interestings are in equine motion analysis, motor control, motor learning, fuzzy logic, neural networks, and system modeling. He can be reached at shadaoha@cvm.msu.edu.

Jim Patton is a research assistant professor in the Robotics Lab at the Sensory Motor Performance Program of the Rehabilitation Institute of Chicago. He can be reached at j-patton@northwestern.edu.

Ferdinando. A. Mussa-Ivaldi is a professor of Northwestern University, USA. He can be reached at sandro@northwestern.edu.